ELSEVIER

Analysis of the enantioselectivities and initial rates of the hydrosilylation of acetophenone catalyzed by [Rh(cod)Cl]₂/(chiral diphosphine). The quantitative analysis of ligand effects

Clementina Reyes, Alfred Prock *, Warren P. Giering *

Department of Chemistry, Metcalf Science and Engineering Center, Boston University, Boston, MA 02215, USA

Abstract

Through the application of the quantitative analysis of ligand effects (QALE) method to the study of the hydrosilylation of acetophenone, we have shown, for the first time, that the initial rate and enantioselectivity of a complicated catalytic system responds in a rational manner to the variations in the stereoelectronic properties of the silane. The reactions (in benzene-d_6 at 63 °C) were catalyzed by [Rh(cod)Cl]₂/(chiral diphosphine) (chiral diphosphine = (R)-BINAP [(R)-(+)-2,2′-bis(diphenylphosphino)-1,1′binaphthyl], (R,R)-tolyl-BINAP [(R)-(+)-2,2′-bis(di-p-tolylphosphino)-1,1′-binaphthyl], (R,R)-Me-DUPHOS [(R,R)-(−)-1,2-Bis-2,5-dimethylphospholano)benzene], (R,R)-DIOP [(R,R)-(−)-2,3-O-isopropylidine-2,3-dihydroxy-1,4-bis(diphenylphosphino)butane], and (R)-QUINAP [(R)-(+)-1-(2-diphenylphosphino-1-naphthyl)isoquinoline]. The ee's (R) of the hydrosilylation products (CH₃CH(OSiR₃)Ph) range between −9 and 53% with the (R)-QUINAP giving the poorest enantioselectivity. The QALE analyses of log(R/S) for (R)-BINAP, (R)-tolyl-BINAP, (R,R)-Me-DUPHOS, and (R,R)-DIOP reveal that the steric effects associated with the silanes are not monotonic.
© 2003 Elsevier Science B.V. All rights reserved.

Keywords: Asymmetric catalysis; Ketone; Hydrosilylation; Kinetics; Ligand effects; Quantitative analysis of ligand effects

1. Introduction

The demand, utility, and commercial value of single isomer materials has fueled the explosive growth of catalytic asymmetric syntheses. A survey of the 2073 chiral ligands and over 13,000 enantioselective reactions listed in Brunner and Zettlmeier's *Handbook of Enantioselective Catalysis* [1] reveals that most of these catalytic reactions give only modest stereoselectivity and only very few give stereoselectivities that approach 100%. In a recent review, Vogl et al. [2] point out that although 90–95% enantioselectivities have been achieved in the laboratory, this is usually not sufficient for the pharmaceutical industry where certification requires enantiomeric purity of greater than 99%. Hence, the transference of asymmetric catalytic reactions to industry has been slow. They also go on to note

that the improvement of asymmetric catalysis appears 'to be modern alchemy'. Bosnich has also been noted that 'It is somewhat disconcerting that after > 20 years of intensive study, success in asymmetric catalysis is largely dependent on a mixture of luck, intuition, and perseverance' [3]. In fact, in order to achieve the most efficacious asymmetric catalyst, the chemical community has focused on synthesizing chiral ligands with the expectation that luck and intuition will lead to at least one member of the set that will give high stereoselectivity for a given reaction. The problem is that variables such as the charge and oxidation state of the metal, chiral ligand, solvent, substrate, and temperature as well as added enhancers all can profoundly influence the outcome of a catalytic reaction. Obviously, the number of possible combinations is enormous.

Consider the catalytic hydrosilylation of ketones (Scheme 1) [4–10]. The reaction, which is an attractive alternative to high pressure catalytic hydrogenation, is technically simple, is readily scaled up, and yields

* Corresponding authors.
E-mail address: prock@bu.edu (A. Prock).
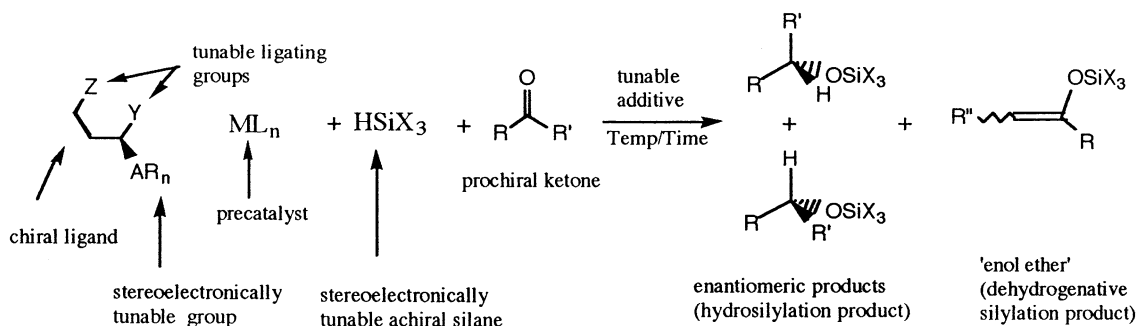
Scheme 1.

directly protected alcohols in the form of silylethers, which are easily converted to the alcohols. The ee's for this reaction range from a few percent to $>90\%$ depending on the catalyst and chiral ligand [1].

This reaction has been extensively studied in terms of metals, chiral ligands, silanes, stereoselectivities, chemoselectivity, solvent, and mechanism. Despite all this effort, this reaction has not yet lived up to its full potential. This asymmetric catalytic reaction generally gives modest enantioselectivities although enantionselectivities as high 99% have been reported [1,9]. It is often accompanied by the undesired extensive dehydrogenative hydrosilylation to form the silylenol ethers. The tertiary silanes react sluggishly, raising the problem of catalyst degradation over long reaction times.

Catalytic hydrosilylation does offer the luxury of having separately tunable components most notably the chiral ligand, the silane, and additives. These ideas are illustrated in Scheme 1 (vide supra). Thus, it is possible that we could tune the stereoselectivity of this reaction by rationally manipulating these components. But even if we perform a study where we keep the metal, chiral ligand, solvent, temperature, ketone and additive constant and vary only the silane, we are dealing with a library of silanes that numbers in the thousands. (The number of possibilities is mind boggling when the other components are considered as well.) In principle, the number of combinations can be reduced via the quantitative analysis of ligand effects method (QALE, vide infra) where analysis of the data for a handful of silanes can be used to predict the properties of a large library of reactants.

As far as we know there have been no reports of studies showing that enantioselectivities of a catalytic reaction respond in a quantifiable manner to variations in the stereoelectronic properties of any of the reactants. It is the purpose of this study to test if such a quantification is possible for a system as complicated as the catalytic hydrosilyation of ketones. The generally low enantioselectivities of this reaction is actually a desirable property because, in principle, statistically significant changes in enantioselectivities can be observed.

2. Systematic studies of the hydrosilylation of ketones

We found in the literature only a few quantitative and systematic studies of the stereoselectivity of hydrosilylation reactions as a function of either the stereoelectronic properties of the chiral ligand or other reactants. Most of these studies are of the Hammett type [11–17]. The most extensive study was reported by Kagan et al.; unfortunately, a quantitative analysis of the stereoselectivities is not possible since the data were collected at different temperatures [16]. Only a handful of reports describe systematic (but still qualitative) examinations of the ligands or silanes [8,18–20]. The only relevant QALE analyses were performed by Marciniec and coworkers [21,22] who found that the rate of oxidative-addition of silanes to $RhCl(cod)PPh_3$ as well as the rate of hydrosilylation of 1-hexene could be described in terms of the QALE model (vide infra). In their study of the rhodium catalysis of the hydrosilylation of ketones, Waldman et al. found that the stereoselectivity and rate were dependent on the nature of added monophosphine as well as silane [8]. Ito et al. have used derivatized TRAP ligands in the hydrosilylation of a variety of ketones [23]. None of these aforementioned studies report data amenable to quantitative analysis. In related studies, we have shown that the QALE model can be used to interpret the dihydroxylation of chiral allyl silanes [24] and the hydride addition to cationic iron carbene complexes [25].

Herein, we report the results of our study of the hydrosilylation of acetophenone (Scheme 2) in which we sought to answer the question 'Can the QALE model be used to interpret the results of a chiral catalytic reaction.' The answer, as we will see, is a resounding yes.

3. Experimental

3.1. General considerations

The following compounds were purchased from Aldrich, United Chemical Technologies, and STREM: (R)-BINAP   [(R)-(+)-2,2′-bis(diphenylphosphino)-
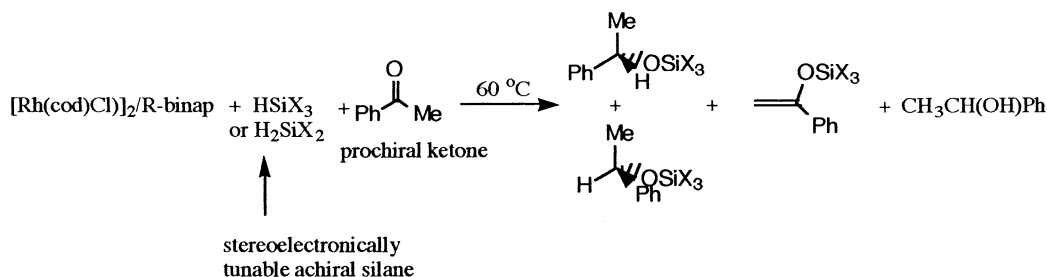
Scheme 2.

1,1′binaphthyl] 99%/HPLC, (R,R)-DIOP [(R,R)-$(-)$-2,3-O-Isopropylidine-2,3-dihydroxy-1,4-bis(diphenyl-phosphino)butane] 98%, (R)-tolyl-BINAP [(R)-$(+)$-2,2′-bis(di-p-tolylphosphino)1,1′-binaphthyl] 98%, (R,R)-Me-DUPHOS [(R,R)-$(-)$-1,2-bis(($2R,5R$)-2,5-dimethylpholano)benzene] 99%, (R)-acetyl mandelic acid (98%ee/GLC), Bu3SiH, Pr3SiH, EtMe2SiH, Et2MeSiH, CyMe2SiH, Et3SiH, MePhSiH2, Ph2Me-SiH, Et2SiH2, Ph2SiH2, Ph3SiH, acetophenone-d3, and acetophenone. All the silanes and acetophenone were distilled or recrystallized prior to use and were stored under an argon atmosphere. The identity of the silanes was verified by NMR spectroscopy. (p-ClC6H4)3SiH, (p-CF3C6H4)3SiH, (p-MeC6H4)3SiH, (p-MeOC6H4)3-SiH, n-Bu2SiH2 and Cy2SiH2 were synthesized using the procedure described below. Rhodium trichloride was obtained from Alfa Aesar and from the generous donation of Professor Pericles Stavropoulos (Boston University). Benzene-d_6 was purchased from Cambridge Isotopes and was dried using molecular sieves and stored in a desiccator. [Rh(cod)Cl]2 was prepared following the procedure of Crabtree and Giordano [26] (p-XC6H4)3SiH (X = OMe, CF3) and H2SiR2 (R = Bu, cyclohexyl) were prepared as described by Benkeser and Riel [27] and West and Rochow [28], respectively.

3.2. Hydrosilylation of acetophenone

To a 10-ml Schlenk flask connected to a vacuum line were added (R)-BINAP (0.0041 M, 0.0025 g), benzene-d_6 (to make the total volume of the reaction 1 ml), Bu3SiH (0.82 M, 211 ml), and acetophenone (0.41 M, 48 ml). The mixture was freeze–pump–thaw degassed after each addition using liquid nitrogen. After these reactants were added, the mixture was allowed to stand for 1 h at room temperature (r.t.) under an argon atmosphere. During that time, [Rh(cod)Cl]2, (0.0041 M in Rh, 1 mg) was weighed into a separate tube and purged with argon. Then the mixture was added to [Rh(cod)Cl]2 and immediately transferred to a previously argon purged NMR tube containing an internal standard. The standard was 7 ml of trichloroethylene in a sealed 10 micro-pipette tube (Drummond Scientific Company). The NMR tube containing the mixture was promptly placed

in a dry-ice acetone bath (-78 °C) and then connected to a vacuum pump via Swagelok connection where it was subjected to four cycles of freeze–pump–thaw degassing before being flame-sealed. After taking the initial measurement of the reaction, the tube was placed in a water bath at 63 °C. The absolute yields of the products and the amount of residual reactants in the final reaction mixtures were determined by ^{1}H-NMR spectroscopy by comparison of the integrations of the appropriate resonances to the that of the internal standard.

3.3. Kinetic studies

Kinetic studies were performed as described elsewhere [29].

3.4. Hydrolysis of $CH_3CH(OSiR_3)Ph$

The reaction was terminated when it was complete or showed no further progress. No attempt was made to separate the final products (CH3CH(OSiR3)Ph, CH3CH(OH)Ph and CH2=CH(OSiR3)Ph). The final reaction mixture was hydrolyzed using a modification of the procedure reported by Guillard and Morton [30]. The NMR tube was opened and the solution transferred to a 25-ml round bottom flask. Benzene-d_6 was evaporated and 1.23 mmol (three equivalents) of tetrabuty-lammonium fluoride in 1.5 ml tetrahydrofuran was added to the residue. The solution was stirred for 24 h at r.t. before 2.5 ml of saturated aqueous NH4Cl solution was added. After the addition of the NH4Cl solution, the solution was stirred for another 3 h. The organic layer was extracted three times with 10 ml of ethyl acetate and the combined extracts were dried overnight over MgSO4. Filtration followed by evaporation of the filtrate gave a yellowish oil, which was then passed through a plug of silica gel (3 cm high) using a 90:10 petroleum ether–ethyl acetate solution. The solvent was evaporated. The NMR spectrum of the residue taken in benzene-d_6 showed only the presence of acetophenone and 1-phenylethanol.

3.5. Determination of the enantiomeric purity of CH₃CH(OH)Ph

The procedure followed was described by Panek and Sparks [31]. The mixture of (R)-CH₃CH(OH)Ph and (S)-CH₃CH(OH)Ph obtained from the hydrolysis of CH₃CH(OSiR₃)Ph was added to 3 ml of freshly distilled methylene chloride. The mixture was transferred to a 25-ml round bottom flask containing (R)-acetyl mandelic acid (1.3 equivalents, 0.1034 g). This flask was placed in an ice-bath before adding dicyclohexylcarbodiimide (DCC), (1.206 equivalents, 0.1020 g), and 4-dimethyla-minopyridine (DMAP) (0.090 mmol, 0.011 g). The reaction was stirred at r.t. for 48 h. The resulting mixture of diastereomers was purified by passing the mixture through a plug of silica gel (∼ 3 cm high) using a 90:10 petroleum ether–ethylacetate solution. Evapora-tion of the solvent gave the diastereomeric esters with a 100% conversion. The ratio of the diastereomers was determined by ¹H-NMR spectroscopy. The error was estimated to be ±1%.

3.6. The QALE model[1]

We and others [32–52] have correlated a large body of data (over 400 sets of thermodynamic, electrochemical, kinetic, stereochemical (vide infra), bond length, UV, IR, NMR, PES, Mossbauer data) with the four stereo-electronic parameters (χ_d, θ, E_{ar} and π_p) via the following QALE equation and its variants (Eq. (1)).

$$\text{property} = a\chi_d + b\theta + b'(\theta - \theta_{st})\lambda + cE_{ar} + d\pi_p + e \quad (1)$$

χ_d describes the s donor capacity of the ligand; θ is Tolman's cone angle; θ_{st} is the steric threshold, which is the cone angle where the steric effect changes; λ is the switching function which equals zero when θ is less than θ_{st} and equals one when θ is equal to or greater than θ_{st}; E_{ar} is a secondary electronic parameter originally thought to be associated with aryl groups but has now been found to be more general; and π_p is a parameter that describes the π acidity of the ligand. This general form of the QALE equation allows for a steric threshold with a steric effect on the low θ side and a different steric effect on the high θ side of the steric threshold. We and others have demonstrated the transferability of the phosphorus stereoelectronic parameters to silanes and silyl groups [21,22,24,53,54].

---

[1] See our QALE web site (www.bu.edu/qale) for a full description of the QALE model.

4. Results and discussion

We have studied the catalytic hydrosilylation of acetophenone using the [Rh(cod)Cl]₂/(chiral dipho-sphine) system in benzene-d_6 at 63 °C. Both secondary and tertiary silanes were employed. The rates of the reactions with secondary silanes were too fast to measure at 63 °C. The product distributions, initial rates and ee's were found to be dependent on both the nature of the silane and the chiral diphosphine ligand. The data are presented in Table 1. The (R)-BINAP, (R)-tolyl-BINAP, (R,R)-Me-DUPHOS and (R,R)-DIOP systems give generally high yields of CH₃CH(OSiR₃)Ph accom-panied by the formation of smaller amount of the dehydrogenative hydrosilylation product (CH₂=CH(O-SiR₃)Ph and still smaller amounts of 1-phenylethanol. The combined 1-phenylethanol formed during the hydrosilylation reaction and the 1-phenylethanol formed by hydrolysis of CH₃CH(OSiR₃)Ph exhibited ee's that spanned a range of −5 to 50%. (R)-QUINAP on the other hand gave highly variable yields of (CH₂=CH(OSiR₃)Ph and CH₃CH(OSiR₃)Ph, which had ee's that were small and showed no particular pattern.

4.1. Insights into the mechanism of hydrosilylation via the QALE model

The most commonly accepted mechanism for the hydrosilyation of ketones was proposed by Ojima nearly thirty years ago (Scheme 3) [55]. Kolb and Hetflejs' [56] kinetic study of the hydrosilylation of t-butylphenyl ketone by diphenylsilane using [{Rh(−)(diop)}]⁺ClO₄⁻ largely supports this mechanism. Significantly, they observed a saturation effect as the concentration of the ketone was increased. In their view, this observation suggested that prior to the oxidative-addition of the silane (Scheme 3) there is reversible complexation of the ketone that deactivates the rhodium. Waldman et al. also observed that the rate of hydrosilylation of 2,2-dimethylcyclopentanone with Rh(diphos)(PPh₃)₂⁺ (PF₆⁻ or BF₄⁻) is first-order in both silane and catalyst but is independent of ketone concentration for [ketone] > 0.5 M [8]. They also suggested that the ketone adds to the rhodium before the oxidative-addition of the silane. Zheng and Chan studied the rhodium catalyzed hydro-silylation of α,β-unsaturated carbonyl compounds [57]. They concluded that the Ojima mechanism could not account for their observation that tertiary silanes give 1,2-addition, whereas, primary and secondary silanes give 1,4-addition. They also observed no significant kinetic isotope effect, suggesting that neither the oxida-tive addition of the silane or the elimination of the silyl ether from the rhodium complex could be the turnover limiting step. They went on to suggest that the turnover limiting step is the coordination of the ketone with a silylhydridorhodium species.

Table 1
Chiral ligands and silanes used in the hydrosilylation of acetophenone catalyzed by [Rh(cod)Cl]$_2$ in benzene-d_6 at 63 °C

#	Chiral Ligand log(Initial Rates/Md^{-1})	H-SiZ$_3$	% CH$_3$CH(OSiR$_3$)Ph	% CH$_2$=C(OSiR$_3$)Ph	% CH$_3$CH(OH)Ph	e.e. (R/S) CH$_3$CH(OH)Ph
	(R)-BINAP, PPh$_2$ / PPh$_2$					
1		-SiHEt$_2$	82	18	0	22
2		-SiHPhMe	84	16	0	46
3		-SiHBu$_2$	85	15	0	27
4		-SiPhMe$_2$	90	7	1	4
5	0.097	-SiEtMe$_2$	92	4	1	-5.0
6		-SiHPh$_2$	70	29	1	34
7		-SiEt$_2$Me	88	4	4	0.2
8	-0.894	-SiEt$_3$	83	4	7	8
9	-0.399	-Si(i-Pr)Me$_2$	74	5	5	4
10	-0.886	-SiPr$_3$	83	6	10	11
11	-0.630	-SiCyMe$_2$	88	4	7	9
12	-0.790	-SiBu$_3$	86	7	3	14
13		-SiPh$_2$Me	91	7	0	4
14		Si(C$_6$F$_5$)Me$_2$	92	7	0	10
15		-Si(i-Bu)$_3$	NR			
16		-SiHCy$_2$	-	-	-	47
17		-Si(p-MeOC$_6$H$_4$)$_3$	80	0	4	-2.3
18	-0.488	-SiPh$_3$	92	4	1	-1.5
19	0.109	-Si(p-ClC$_6$H$_4$)$_3$	-	-	-	-
20	0.546	-Si(p-F$_3$CC$_6$H$_4$)$_3$	98	1	0	-0.8
21		-SiH(t-Bu)$_2$	85	15	0	7
22		-Si(i-Pr)$_3$	NR			
	P(p-MeC$_6$H$_4$)$_3$ / P(p-MeC$_6$H$_4$)$_3$					
23		-SiHEt$_2$	86	14	0	33
24		-SiHPhMe	86	14	0	53
25		-SiHBu$_2$	89	11	0	33
26		-SiPhMe$_2$	96	1	2	-1
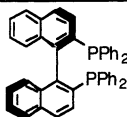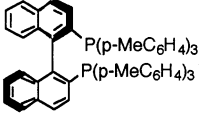
Table 1 (*Continued*)

27	-SiEtMe$_2$	92	3	1	4
28	-SiHPh$_2$	75	25	0	32
29	-SiEt$_3$	84	5	7	7
30	-SiPr$_3$	81	6	7	11
31	-SiCyMe$_2$	90	4	5	10
32	-SiBu$_3$	80	9	8	11
33	-SiPh$_2$Me	93	6	0	0
34	Si(C$_6$F$_5$)Me$_2$	92	5	0	8
35	-SiPh$_3$	92	4	1	-1.0
36	-Si(p-F$_3$CC$_6$H$_4$)$_3$	97	1	0	2.5
37	-SiH(t-Bu)$_2$	93	7	0	3
38	-SiHEt$_2$	99	1	0	36
39	-SiHPhMe	99	1	0	41
40	-SiHBu$_2$	99	0	0	35
41	-SiPhMe$_2$	89	0	0	-4
42	-SiEtMe$_2$	75	0	1	-10
43	-SiHPh$_2$	99	1	0	36
44	-SiEt$_2$Me	84	0	1	-8
45	-SiEt$_3$	79	0	5	3
46	-SiPr$_3$	74	1	3	-2.3
47	-SiCyMe$_2$	95	0	0	-7.7
48	-SiBu$_3$	99	0	0	-0.3
49	-SiPh$_2$Me	96	0	0	0.6
50	Si(C$_6$F$_5$)Me$_2$	97	2	0	35
51	-SiPh$_3$	71	0	0	-1.1
52	-Si(p-F$_3$CC$_6$H$_4$)$_3$	94	2	0	2.7
53	-SiH(t-Bu)$_2$	86	10	0	7
54	-SiHEt$_2$	70	30	0	45
55	-SiHPhMe	93	7	0	32
56	-SiHBu$_2$	61	39	0	35
57	-SiPhMe$_2$	54	0	0	7
58	-SiEtMe$_2$	60	10	0	6
59	-SiHPh$_2$	96	4	0	24
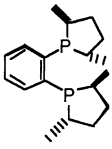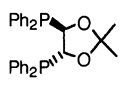
Table 1 (*Continued*)

60	-SiEt$_2$Me	90	5	1	6
61	-SiEt$_3$	70	4	1	9
62	-SiPr$_3$	98	1	1	8
63	-SiCyMe$_2$	90	5	1	8
64	-SiBu$_3$	91	5	3	10
65	-SiPh$_2$Me	66	6	1	3
66	Si(C$_6$F$_5$)Me$_2$	84	10	2	4
67	-SiPh$_3$	90	2	1	2.4
68	-Si(p-F$_3$CC$_6$H$_4$)$_3$	90	3	0	-3.9
69	-SiH(t-Bu)$_2$	83	17	0	27
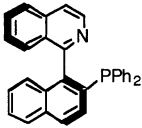
70	-SiHEt$_2$	18	82	0	0
71	-SiHPhMe	62	38	0	10
72	-SiHBu$_2$	30	70	0	9
73	-SiPhMe$_2$	52	46	0	5
74	-SiEtMe$_2$	50	49	0	3
75	-SiHPh$_2$	46	54	0	7
76	-SiEt$_2$Me	64	24	1	4
77	-SiEt$_3$	65	8	1	7
78	-SiPr$_3$	95	1	1	6
79	-SiCyMe$_2$	80	14	2	5
80	-SiBu$_3$	92	5	0	4
81	-SiPh$_2$Me	62	15	0	
82	-Si(C$_6$F$_5$)Me$_2$	84	8	0	5
83	-SiPh$_3$	65	16	1	-9
84	-Si(p-F$_3$CC$_6$H$_4$)$_3$	79	3	0	7
85	-SiH(t-Bu)$_2$	81	15	0	1

The yields of CH$_3$CH(OSiR$_3$)Ph, CH$_2$=C(OSiR$_3$)Ph and CH$_3$CH(OH)Ph (formed before hydrolysis) are given in columns 3–6. The ee's of the combined CH$_3$CH(OH)Ph formed during the reaction and by the hydrolysis of CH$_3$CH(OSiR$_3$)Ph are given in the last column.

Recently, we reported the results of an exhaustive kinetic study of the hydrosilylation of acetophenone with HSiBu$_3$ catalyzed by (*R*)-BINAP/[Rh(cod)Cl]$_2$ [29]. The rate of formation of the silylether [PhCH(O-SiR$_3$)CH$_3$] increased linearly with the concentration of HSiBu$_3$, whereas the rate of formation shows a saturation effect as the concentration of acetophenone increases in accordance with the observations of Waldman et al. [8] and Kolb and Hetflejs [56].

Our simulations [29] of the production of PhCH(O-SiR$_3$)CH$_3$ based on the Ojima mechanism, show that this particular model can give a saturation effect without the need to include a deactivating complexation of the ketone. All is that is needed is the turnover limiting oxidative addition of HSiBu3. These simulations and experimental data are shown in Fig. 1.

We now supplement our kinetic study with the QALE analysis of the initial rates of the formation of CH$_3$CH(OSiR$_3$)Ph, Eq. (2). (Data are presented in the first column of Table 1.) We could not obtain initial rates for the secondary silanes because of the high reactivity of these silanes.

Scheme 3.

$$PhC(-O)H_3 + HSiZ_3$$

$$\xrightarrow[\text{Benzene-}d_6 \quad (63\ °C)]{[Rh(cod)Cl]_2/R\text{-}BINAP} PhCH(OSiZ_3)CH_3 \qquad (2)$$
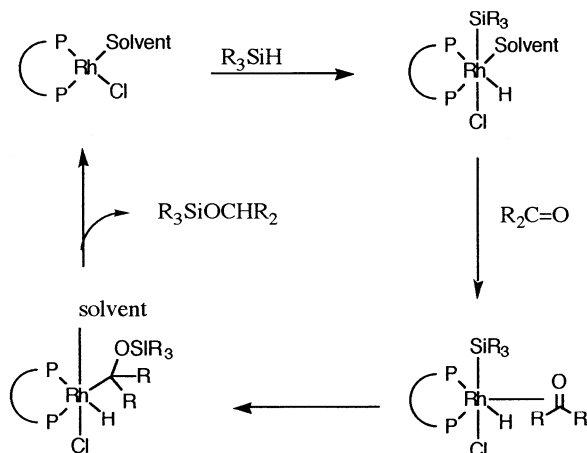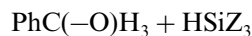
It turns out that the results of this analysis also support the oxidative-addition of the silane to a rhodium complex as the turnover limiting step. We start with graphical analysis of the kinetic data (Fig. 2). In the QALE model, θ, E_{ar} and π_p (see Eq. (1)) are constant for $HSi(p\text{-}XC_6H_4)_3$, with the values 145, 2.7 and 0, respectively. The stereoelectronic parameters of the silanes are listed in Table 2. Thus, a plot of the data versus χ_d for $HSi(p\text{-}XC_6H_4)_3$, affords an estimate (0.14 ± 0.06) of the coefficient of χ_d obtained by regression analysis of the full set of data [32]. This estimate
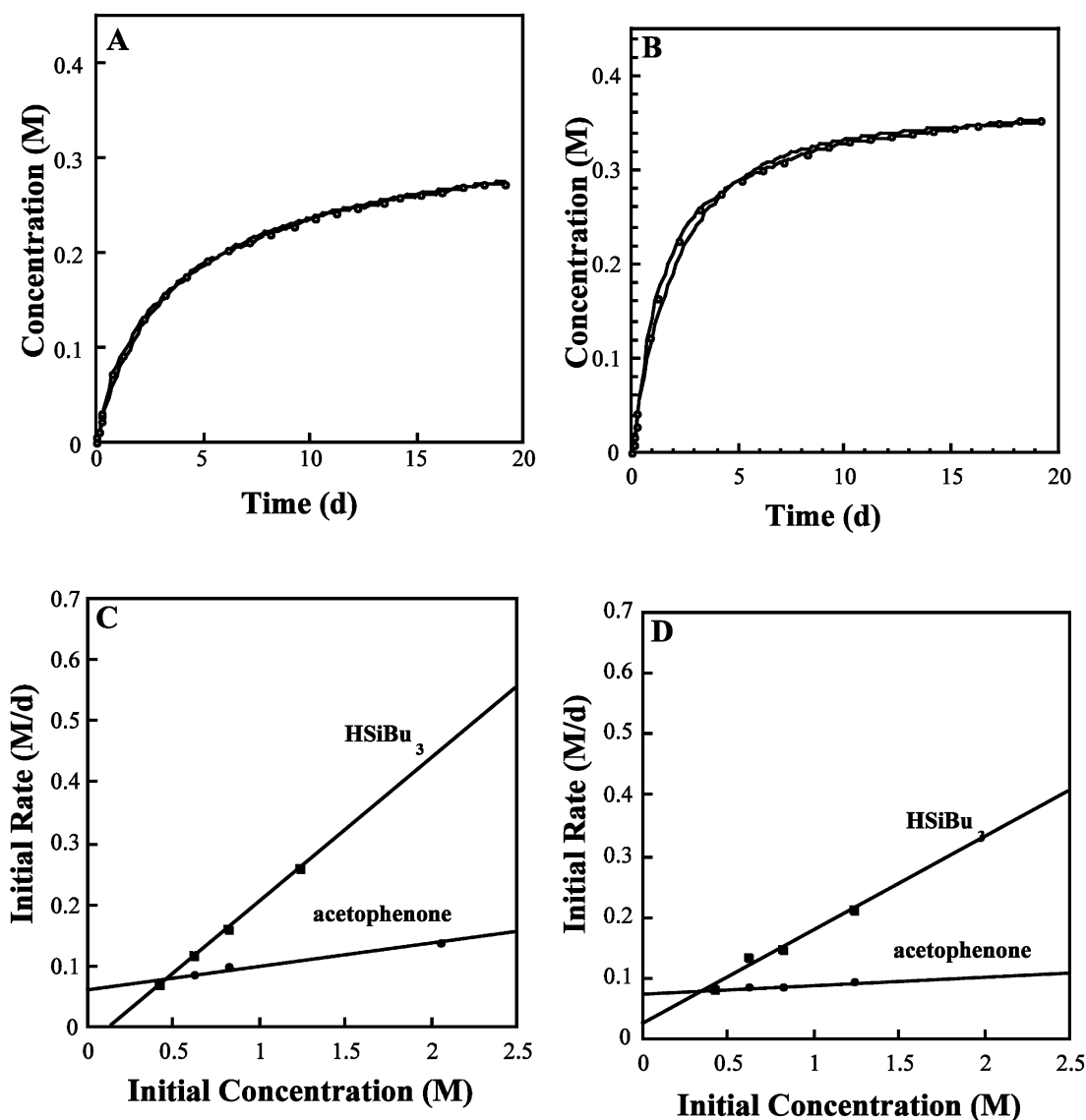
Fig. 1. (A) Simulation and experimental results of the time dependence of the concentration of $PhCH(OSiBu_3)CH_3$ for a nominally 2:1 acetophenone to $HSiBu_3$ mixture. (B) Simulation and experimental results of the time dependence of the concentration of $PhCH(OSiBu_3)CH_3$ for a nominally 1:2 acetophenone to $HSiBu_3$ mixture. In (A) and (B) the experimental points are shown as filled squares. (C) Experimental initial rates of formation of $PhCH(OSiBu_3)CH_3$ as a function of acetophenone and $HSiBu_3$ concentrations. (D) Simulation of the data shown in (C).
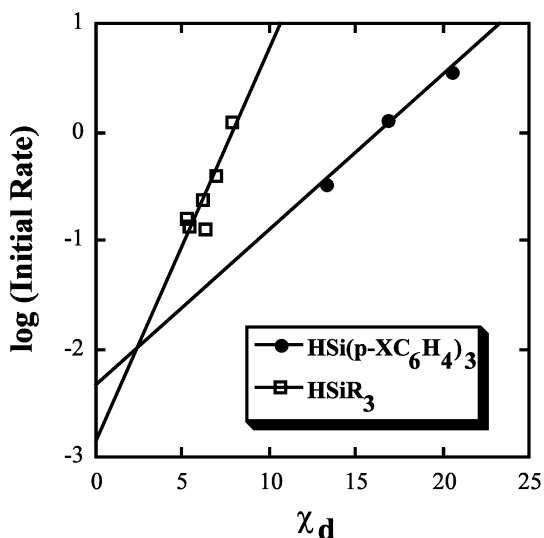
Fig. 2. Plots of log(initial rate) vs. χ_d for HSiR$_3$ and HSi(p-XC$_6$H$_4$)$_3$ in the [Rh(cod)]$_2$/(R-BINAP) catalyzed hydrosilylation of acetophenone.

must be and is statistically indistinguishable from the value (0.13 ± 0.02) obtained for the coefficient of χ_d via regression analysis of the total set. The equivalence of the χ_d coefficients then serves as a check on the full analysis. The positive slope indicates that the poorer electron donor silanes (larger χ_d) react more rapidly.

Insight into the importance of aryl (E_{ar}) and steric effects (θ) can be obtained by combining plots of the data for PR$_3$ with the data for P(p-XC$_6$H$_4$)$_3$ versus χ_d as is shown in Fig. 2 [39]. In the QALE model, only χ_d and

Table 2
The stereoelectronic parameters of the silanes used in this study

No.	HSiZ$_3$	χ_d	θ	E_{ar}	π_p
1	HSiHEt$_2$	9.90	117	0.0	1.2
2	HSiHMePh	12.90	117	1.0	1.2
3	HSiHBu$_2$	9.20	121	0.0	1.2
4	HSiPhMe$_2$	10.60	122	1.0	0.0
5	HsiEtMe$_2$	7.80	123	0.0	0.0
6	HSiHPh$_2$	14.50	126	2.0	1.2
7	HSiEt$_2$Me	7.05	127	0.0	0.0
8	HSiEt$_3$	6.30	132	0.0	0.0
9	HSiMe$_2$(i-Pr)	6.80	132	0.0	0.0
10	HSiPr$_3$	5.40	134	0.0	0.0
11	HSiCyMe$_2$	6.20	135	0.0	0.0
12	HSiBu$_3$	5.25	136	0.0	0.0
13	HSiMePh$_2$	12.60	136	2.2	0.0
14	HSiMe$_2$(C$_6$F$_5$)	17.00	140	1.4	0.0
15	HSi(i-Bu)$_3$	5.7	143	0	0.0
16	HSiHCy$_2$	6.60	144	0.0	1.2
17	HSi(p-MeOC$_6$H$_4$)$_3$	10.50	145	2.7	0.0
18	HSiPh$_3$	13.25	145	2.7	0.0
19	HSi(p-ClC6H4)3	16.8	145	2.7	0.0
20	HSi(p-CF3C6H4)3	20.50	145	2.7	0.0
21	HSiH(t-Bu)2	5.70	150	0.0	1.2
22	HSi(i-Pr)3	3.45	160	0	0.0

The values of the parameters are taken from Ref. [54].

θ vary for HSiR$_3$; furthermore χ_d and θ are linearly related. The larger silanes (larger θ) are better electron donors (smaller χ_d). Since the positive slope of the line defined by the data for HSiR$_3$ is steeper than the line defined by P(p-XC$_6$H$_4$)$_3$ we see that θ is playing a significant inhibitory role. An important consequence of the linear correlation between χ_d and θ for PR$_3$ is that when there is no E_{ar} effect, the line for the isosteric P(p-XC$_6$H$_4$)$_3$ ligands with $\theta = 145°$ crosses the line for PR$_3$ at $\chi_d = 4.8$ corresponding also to $\theta = 145°$ for a hypothetical HSiR$_3$. The lines in Fig. 2 cross at a value slightly less than $\chi_d = 4.8$ suggesting a small E_{ar} effect. The full statistical analysis, however, shows that this effect is not significant. The full regression analysis is displayed in Table 3, entry 5.

The χ_d and θ profiles are shown in Fig. 3. The profile for any parameter is obtained by taking the experimental result and subtracting the calculated contributions of all the parameters except of the one interest. The resulting difference is then plotted versus the parameter of interest. For example, the θ profile would be generated in the following manner

$$\log(\text{initial rate})\theta = \log(\text{initial rate}) - a\chi_d - cE_{ar} - d \quad (3)$$

These profiles give a snapshot of how a property responses to variations in a single parameter. By construction each profile contains the total error.

This QALE analysis is strikingly similar to the QALE analysis of Marciniec's kinetic data for the oxidative-addition of HSiZ$_3$ to [RhCl(cod)(PPh$_3$)] [22,54].

$$\begin{aligned} \text{HSiZ}_3 &+ [\text{RhCl(cod)PPh}_3] \\ &= [\text{RhHCl(cod)(SiZ}_3)\text{PPh}_3] \end{aligned} \quad (4)$$
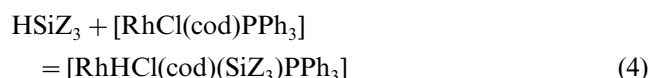
$$\begin{aligned} \log k = (0.098\pm0.004)\chi_d &- (0.038\pm0.005)\theta \\ &+ (0.3\pm0.6) \end{aligned} \quad (5)$$

where $n = 11$, $r^2 = 0.987$ outliers HSi(OEt)$_3$.

For direct comparison, we show below the results of the regression analysis of our data (presented in entry 5 in Table 3) for reaction (2).

$$\begin{aligned} \log(\text{initial rate}) \\ = (0.13\pm0.02)\chi_d &- (0.05\pm0.01)\theta + (5\pm2) \end{aligned} \quad (6)$$

where $n = 9$, $r^2 = 0.923$

The results of this QALE analysis, like the analysis of the Marciniec data, are consistent with our early assertion [29] (based on kinetic data) that the oxidative-addition of the silane to a rhodium complex is the turnover limiting step in the R-BINAP system. We cannot reconcile our results with the results of the deuterium isotope effects. Clearly, this issue is deserving of further study.

Table 3
The regression coefficients (Eq. (1)) and statistics that result from the QALE analyses of the enantioselectivities of the [Rh(cod)Cl]$_2$/(chiral ligand) catalyzed asymmetric hydrosilylation of acetophenone

No.	Chiral ligand	Property	a	b	b'	c	d	e	θ_{st}	n	r^2	Outliers
1	(R)-BINAP	log(R/S)	—	0.0113±0.0009	−0.076±0.005	−0.022±0.005	0.28±.01	−1.4±0.1	143	17	0.982	HSiPhMe$_2$, H$_2$SiPhMe
2	(R)-tolyl-BINAP	log(R/S)	—	0.005±0.001	−0.072±0.006	−0.027±0.005	0.25±0.01	−0.6±0.1	144	14	0.985	H$_2$SiPhMe
3	(R,R)-Me-DUPHOS	log(R/S)	—	0.007±0.001	−0.075±0.008	—	0.35±0.02	−0.9±0.2	144	11	0.987	H$_2$SiPhMe
4	(R,R)-DIOP	log(R/S)	−0.0066±0.0008	−0.031±0.003	0.03±0.003	—	0.160±0.007	3.9±0.3	123	14	0.993	H$_2$SiPhMe
5	(R)-BINAP	log(initial rate)	0.13±0.02	−0.05±0.01	—	—	—	5±2	—	9	0.923	—
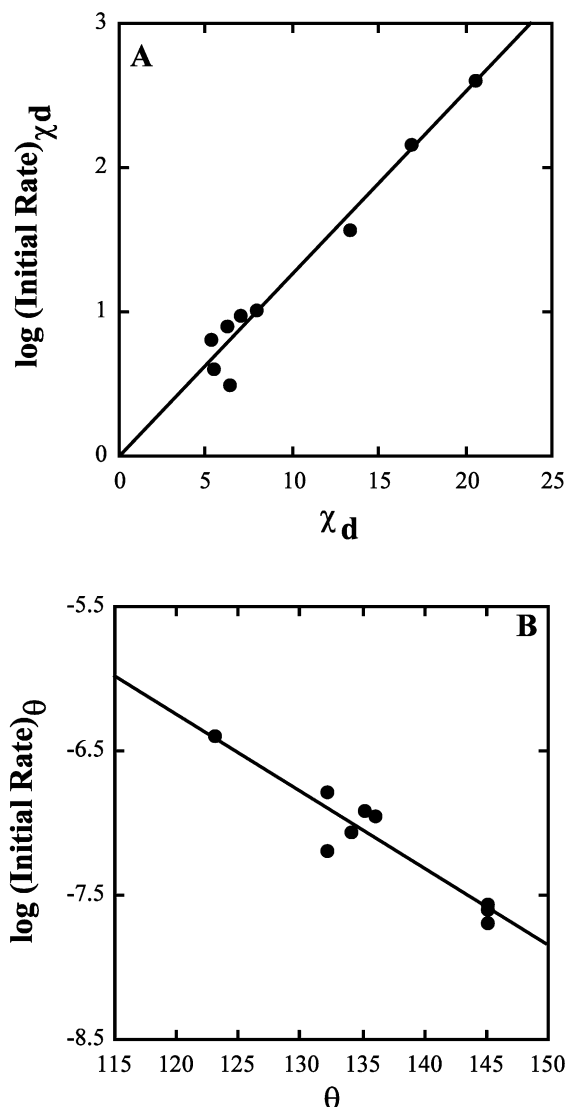
Fig. 3. Electronic and steric profiles for log(initial rate) of the [Rh(cod)]$_2$/R-BINAP catalyzed hydrosilylation of acetophenone.

4.2. QALE analysis of the enantioselectivities (log(R/S)) of the 1-phenylethanol obtained after the hydrolysis of the reaction mixtures

We analyzed, via the QALE model, log(R/S) for the 1-phenylethanol formed after the hydrolysis of the reaction mixtures. We made no attempt to separate the initially formed 1-phenylethanol from the CH$_3$CH(OSiR$_3$)Ph. We do not believe that this influences the overall ee's in a significant way since the yields of the initially formed 1-phenylethanol were generally small. The possible origins of 1-phenylethanol are discussed in reference [29].

To begin our analysis, we plotted log(R/S) versus χ_d for HSiR$_3$ and HSi(p-XC$_6$H$_4$)$_3$ for the (R)-BINAP system (Fig. 4A). The shallow slope of the line defined by the three HSi(p-XC$_6$H$_4$)$_3$ points relative to the line defined by HSiR$_3$ indicates that the electron donor
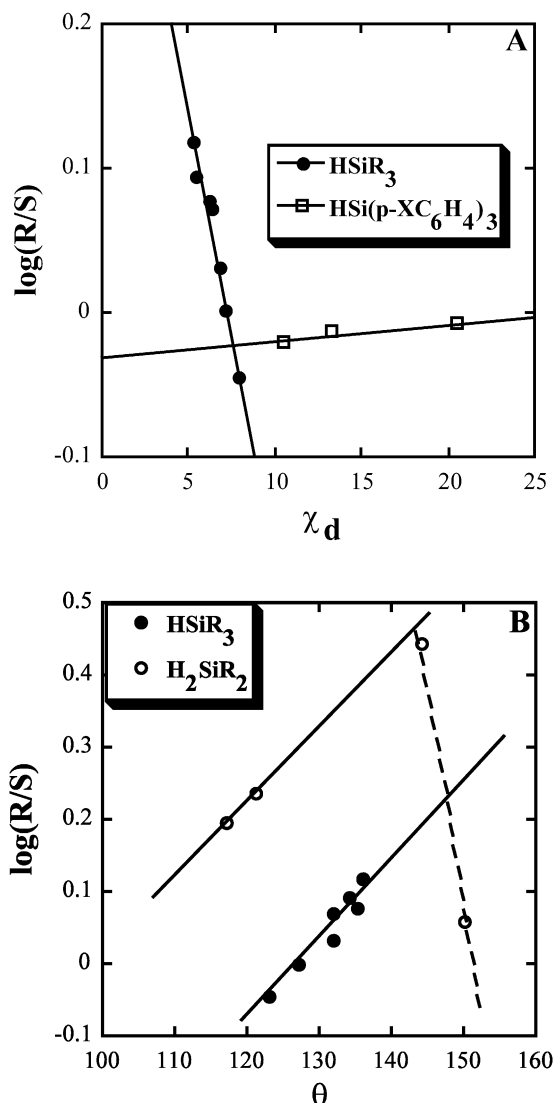
Fig. 4. (A) Plot of $\log(R/S)$ vs. χ_d for the [Rh(cod)]$_2$/(R)-BINAP catalyzed hydrosilylation of acetophenone for HSiR$_3$ and HSi(p-XC$_6$H$_4$)$_3$ (B) Plot of $\log(R/S)$ vs. θ for HSiR$_3$ for H$_2$SiR$_2$. The dashed line in (B) is drawn to suggest the existence of a steric threshold near 143°.

capacity of the silane does not play an important role in determining R/S. The steep slope of the HSiR$_3$ line, however indicates a very significant role for steric effects as is expected for a stereodifferentiating step. The intersection of the two lines is well removed from $\chi_d = 4.8$ (vide supra) thereby indicating a significant Ear effect that diminishes the $\log(R/S)$.

In Fig. 4B, we have plotted $\log(R/S)$ versus θ for the secondary and tertiary alkylsilanes. With the exception of the datum for H$_2$Si(t-Bu)$_2$, the data for the secondary silanes defines a good line. The deviation of H$_2$Si(t-Bu)$_2$ from this line suggests a steric threshold (i.e. there is a change in the influence of size on the property). The data for HSiR3 also define a good line. Unfortunately,

tertiary silanes with $\theta > 136$ were unreactive and we could not further probe the putative steric threshold.

It is noteworthy that the line defined by the tertiary alkylsilanes is significantly separated from the line defined by the secondary alkylsilanes. We know from the analysis of the plots shown in Fig. 4A that χ_d plays only a small role in determining $\log(R/S)$. If only θ and E_{ar} were involved then a plot of $\log(R/S)$ for the secondary and tertiary alkylsilanes versus θ would yield a single line since E_{ar} is zero for both groups of silanes. Therefore, we conclude that the presence of the second Si–H bond in the secondary silanes incrementally enhances the stereoselectively of the reaction. The origins of this incremental effect are obscure. We can express this incremental effect by the inclusion of a parameter that equals the number of hydrogens minus one.

We performed regression analyses, using Eq. (1), for all the systems except the (R)-QUINAP system. The stereoelectronic parameters of the silanes are listed in Table 2. The coefficients and appropriate statistical information for all the analyses are given in Table 3. For the (R)-BINAP system (Table 3, entry 1), we determined that there is, indeed, a steric threshold ($\theta_{st} = 143°$) with steric effects operative on either side of the threshold. The small χ_d effect observed graphically is found to be statistically insignificant for the full set of data. When the ranges of the parameters are considered it follows that the variations in $\log(R/S)$ are dominated by changes in θ and in the number of Si–H bonds.

The steric profile for the (R)-BINAP system is given in Fig. 5A. This profile is quite striking. It shows a region below $\theta = 143°$ where R/S increases as the size of silane increases. A steric threshold is observed at $\theta = 143°$ followed by a region where R/S decreases as the size of the silane increases. There are sufficient data in this set that we can see the curvature as the system transforms from one steric domain to the other. This type of curvature had been anticipated by Poë and coworkers [58] for kinetic data. The (R)-tolyl-BINAP and (R,R)-Me-DUPHOS systems show similar profiles (Fig. 5B,C) and analyses (Table 3, entries 2 and 3).

The question arises as to the origin of steric profiles such as those shown in Fig. 5A–C. The QALE model actually allows for regions of different steric effects; these regions depend on where steric effects turn on in the different transition states or intermediates [59]. In the systems considered herein, we are dealing with two different stereo-differentiating transition states, one that leads to the R isomer of CH$_3$CH(OSiR$_3$)Ph and one that leads to the S isomer. In Fig. 6, we present curves that show how the steric component of $\log k$ for the two stereo-differentiating steps might respond to variations in the size (θ) of the silanes. For very small silanes there should be no steric discrimination between the two transition states (region 'a' in Fig. 6A and B). If the S
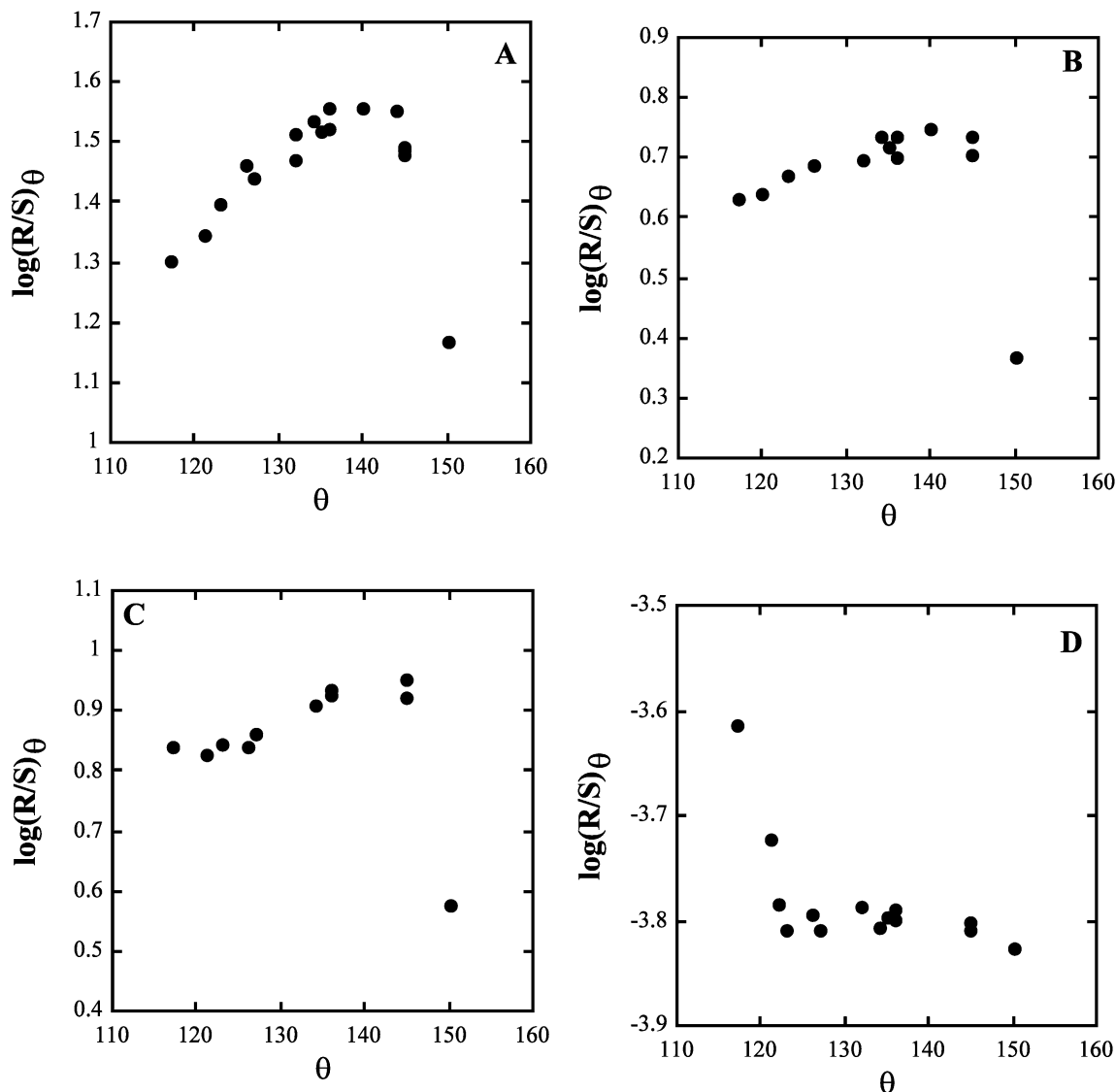
Fig. 5. Plot of $\log(R/S)\theta^a$ vs. θ (steric profiles) for the $[Rh(cod)]_2$ catalyzed hydrosilylation of acetophenone using (A) (R)-BINAP, (B) (R)-tolyl-BINAP, (C) (R,R)-Me-DUPHOS or (D) (R,R)-DIOP.

transition state is more congested than the R transition state, then steric effects will turn on sooner in the S transition state, and the rate of formation of the S isomer will fall (region 'b' in Fig. 6A). Since the rate of formation of the R isomer has not yet been affected by the size of the silane, the R/S ratio will increase (region 'b' in Fig. 6B). At $\theta = 143°$, steric effects become operative in the R transition state and the rate of formation of the R isomer falls (region 'c' in Fig. 6A and B). Since R/S falls after the steric threshold at $\theta = 143°$, it appears that the R transition state is less flexible than the S transition state. (The issue of congestion versus flexibility has been discussed elsewhere [59,60].) Thus, we suggest what we are seeing in Fig. 5A–C are the regions 'b' and 'c' in Fig. 6B.

The result of the analysis of the (R,R)-DIOP system is significantly different from the analyses of the other

chiral phosphines. The regression analysis via Eq. (1) reveals that as the size of the silanes increases, R/S decreases until a steric threshold is reached at $\theta = 123°$. The steric profile (Fig. 5D) shows that after the threshold, R/S appears to become independent of θ. The QALE equation (Table 3, entry 4) describes this behavior by having equal but opposite steric effects after the steric threshold. This behavior is accounted for by the QALE model in the following manner. In this case, after a region of steric effects for the small silanes (region 'a' in Fig. 6C), steric effects turn on first for the more congested R transition state, which results in the preferential formation of the S isomer (region 'b' in Fig. 6C and D). At $\theta = 123°$, steric effects turn on for the S isomer after which its rate of formation declines (region 'c' in Fig. 6C). Since R/S subsequently appears to become independent of θ (region 'c' in Fig. 6D), we
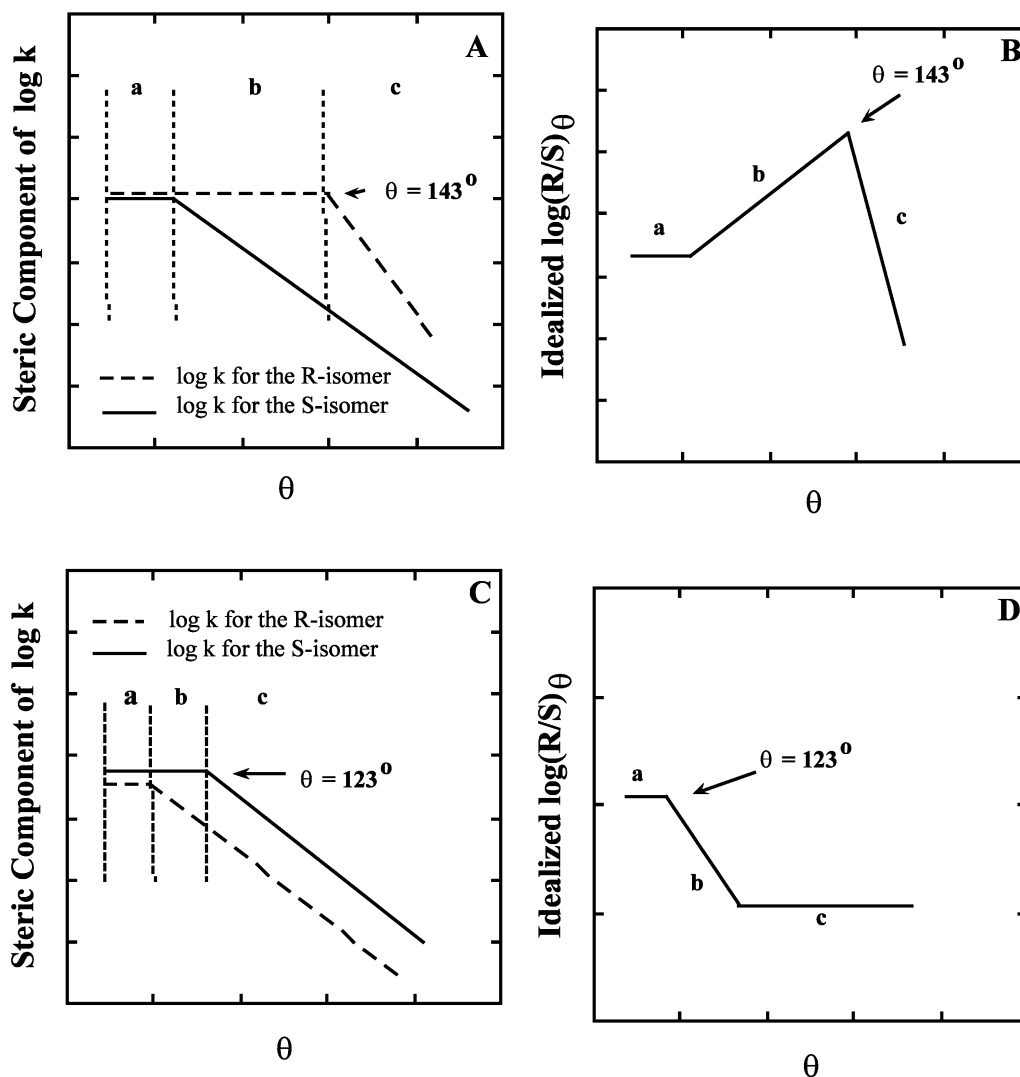
Fig. 6. Cartoons showing how the positions of the respective steric thresholds for the formation of the *R* and *S* isomers of $CH_3CH(OSiR_3)Ph$ determine the shape of steric profiles of the enentioselectivity of the reaction shown in Scheme 2. (A) and (B) refer to the (*R*)-BINAP, (*R*)-tolyl-BINAP and (*R*,*R*)-Me-DUPHOS systems. (C) and (D) refer to the (*R*,*R*)-DIOP system.

envision that the *R* and *S* transition states have similar flexibilities once their respective steric thresholds have been exceeded.

It is curious and potentially important that in all the systems we studied, $H_2SiPhMe$ was an outlier; its stereoselectivity was higher than expected. This deviant behavior might arise because this is the only silane that we studied where the silicon becomes a stereogenic center upon oxidative-addition to the rhodium. This certainly deserves further study.

5. Conclusions

We have demonstrated that the QALE model can be used to analyze the initial rates and enantioselectivities of a catalytic reaction namely, the hydrosilylation of acetophenone. The results of the QALE analysis of the initial rates of this reaction are similar to the results obtained from the QALE analysis of the oxidative addition of silanes to [RhCl(cod)(PPh$_3$)] as reported by Marciniec. These analyses suggest that the turnover limiting step is the oxidative addition of the silane to a rhodium complex. The QALE analysis of the stereo-chemistry of the reaction reveals that steric effects are very non-linear and that monotonically increasing the size of the silane in this asymmetric hydrosilylation of acetophenone does not monotonically increase the enantioselectivity of the reaction.

References

[1] H. Brunner, W. Zettlmeier, Handbook of Enantioselective Catalysis, VCH Publishers, New York, 1993.

[2] E.M. Vogl, H. Groger, M. Shibasaki, Angew. Chem. Int. Ed. Engl. 38 (1999) 1570.

[3] B. Bosnich, Acc. Chem. Res. 31 (1998) 667.

[4] J.D. Morrison, I. Ojima, K. Hirai, Asymmetric Hydrosilylation and Hydrocarbonylation. Aysmmetric Synthesis, Ch. 4, vol. 5, Academic Press, Orlando, FL, 1985.

[5] J.L. Speier, Adv. Organomet. Chem. 17 (1979) 407.

[6] B. Marciniec, J. Gulinski, J. Organomet. Chem. 446 (1993) 15.

[7] B.M. Bode, P.N. Day, M.S. Gordon, J. Am. Chem. Soc. 120 (1998) 1552.

[8] T.E. Waldman, G. Schaefer, D.P. Riley, ACS Symp. Ser. 517 (1993) 58.

[9] I. Ojima, Z. Li, J. Zhu, in: Z. Rappoport, Y. Apeloig (Eds.), Recent Advances in the Hydrosilylation and Related Reactions: Chemistry of Organic Silicon Compounds, vol. 2;, Wiley, New York, 1998, p. 1687.

[10] I. Ojima, in: S. Patai, Z. Rappoport (Eds.), The Hydrosilylation Reaction: the Chemistry of Organosilicon Compounds, Wiley, New York, 1989, p. 1479.

[11] H. Brunner, A. Kurzinger, J. Organometal. Chem. 346 (1988) 413.

[12] T. Ohkuma, H. Ooka, S. Hashiguchi, T. Ikariya, R. Noyori, J. Am. Chem. Soc. 117 (1995) 2675.

[13] T. Hayashi, K. Yamamoto, K. Kasuga, H. Omizu, M. Kumada, J. Organomet. Chem. 113 (1976) 127.

[14] Y. Nishibayashi, J.D. Singh, Y. Arikawa, S. Uemura, M. Hidai, J. Organomet. Chem. 531 (1997) 13.

[15] R. Noyori, S. Hashiguchi, Acc. Chem. Res. 30 (1997) 97.

[16] J.F. Peyronel, J.C. Fiaud, H.B. Kagan, J. Chem. Res. M (1980) 4057.

[17] M.B. Carter, B. Sechiott, A. Gutierrez, S.L. Buchwald, J. Am. Chem. Soc. 116 (1994) 11667.

[18] I. Matsuda, Y. Fukuta, T. Tsuchihashi, H. Nagashima, K. Itoh, Organometallics 16 (1997) 4327.

[19] B.T. Gregg, A.R. Cutler, J. Am. Chem. Soc. 118 (1996) 10069.

[20] J. Halpern, P.F. Phelan, J. Am. Chem. Soc. 94 (1972) 1881.

[21] W. Duczmal, B. Maciejewska, E. Sliwinska, B. Marciniec, Transition Met. Chem. 20 (1995) 162.

[22] W.S. Duczmal, B. Maciejewska, B. Marciniec, H. Maciejewski, Transition Met. Chem. 20 (1995) 435.

[23] R. Kuwano, M. Sawamura, J. Shirai, M. Takahashi, Y. Ito, Bull. Chem. Soc. Jpn. 73 (2000) 485.

[24] B.A. Lorsbach, A. Prock, W.P. Giering, Organometallics 14 (1995) 1694.

[25] B.A. Lorsbach, D.M. Bennett, A. Prock, W.P. Giering, Organometallics 14 (1995) 869.

[26] R.H. Crabtree, G. Giordano, Inorg. Syn. 19 (1976) 218.

[27] R.A. Benkeser, J.F. Riel, J. Am. Chem. Soc. 73 (1951) 3472.

[28] R. West, E.G. Rochow, J. Org. Chem. 18 (1953) 303.

[29] C. Reyes, A. Prock, W.P. Giering, Organometallics 21 (2002) 546.

[30] J.W. Guillard, R. Fortin, H.E. Morton, C. Yoajim, C.A. Quesnelle, S. Daignault, Y. Guindon, J. Org. Chem. 53 (1988) 2606.

[31] J.S. Panek, M.A. Sparks, Tetrahedron: Asymmetry 1 (1990) 801.

[32] M.R. Wilson, D.C. Woska, A. Prock, W.P. Giering, Organometallics 12 (1993) 1742.

[33] M.R. Wilson, H. Liu, A. Prock, W.P. Giering, Organometallics 12 (1993) 2044.

[34] A.A. Tracey, K. Eriks, A. Prock, W.P. Giering, Organometallics 9 (1990) 1399.

[35] J. Panek, A. Prock, K. Eriks, W.P. Giering, Organometallics 9 (1990) 2175.

[36] A.L. Fernandez, C. Reyes, M.R. Wilson, D.C. Woska, A. Prock, W.P. Giering, Organometallics 16 (1997) 342.

[37] A.L. Fernandez, A. Prock, W.P. Giering, Organometallics 15 (1996) 2784.

[38] A.L. Fernandez, A. Prock, W.P. Giering, Organometallics 13 (1994) 2767.

[39] J. Bartholomew, A.L. Fernandez, B.A. Lorsbach, M.R. Wilson, A. Prock, W.P. Giering, Organometallics 15 (1996) 295.

[40] A.J. Poe, R.H.E. Hudson, Organometallics 14 (1995) 3238.

[41] A.J. Poe, D.H. Farrar, Y. Zheng, J. Am. Chem. Soc. 114 (1992) 5146.

[42] A. Neubrand, A.J. Poe, R. van Eldik, Organometallics 14 (1995) 3249.

[43] Farrar, D.H.; Poe, A.J.; Zheng, Y.J. Am. Chem. Soc. 1994, 116, 6252.

[44] L.Z. Chen, A.J. Poe, Coord. Chem. Rev. 143 (1995) 265.

[45] N.M.J. Brodie, A.J. Poe, Can. J. Chem. 73 (1995) 1187.

[46] R. Romeo, G. Arena, L.M. Scolaro, Inorg. Chem. 31 (1992) 4879.

[47] X. Luo, G.J. Kubas, C.J. Burns, J.C. Bryan, C.J. Unkefer, J. Am. Chem. Soc. 117 (1995) 1159.

[48] C.A. Bessel, J.A. Margarucci, J.H. Acquaye, R.S. Rubino, J. Crandall, A.J. Jircitano, K.J. Takeuchi, Inorg. Chem. 32 (1993) 5779.

[49] C. Moreno, M.J. Macazaga, S. Delgado, Organometallics 10 (1991) 1124.

[50] R.S. Herrick, R.R. Duff, Jr, A.B. Frederick, J. Coord. Chem. 32 (1994) 103.

[51] D.H. Farrar, J. Hao, A.J. Poe, T.A. Stromnova, Orgnaometallics 16 (1997) 2827.

[52] R. Romeo, G. Alibrandi, Inorg. Chem. 36 (1997) 4822.

[53] D.M. Hester, J. Sun, A.W. Harper, G.K. Yang, J. Am. Chem. Soc. 114 (1992) 5234.

[54] www.bu.edu/qale

[55] I. Ojima, T. Kogure, M. Kumagai, S. Horiuchi, Y. Sato, J. Organometal. Chem. 122 (1976) 83.

[56] I. Kolb, J. Hetflejs, Coll. Czech. Chem. Commun. 45 (1980) 2808.

[57] G.Z. Zheng, T.H. Chan, Organometallics 14 (1995) 70.

[58] K. Dahlinger, F. Falcone, A.J. Poe, Inorg. Chem. 25 (1986) 2654.

[59] E. Eriks, H.-Y. Liu, A. Prock, W.P. Giering, Inorg. Chem. 28 (1989) 1759.

[60] M.N. Golovin, M.M. Rahman, J.E. Belmonte, W.P. Giering, Organometallics 4 (1985) 1981.